Dielectric Constants of Silicon Quantum Dots

Lin-Wang Wang and Alex Zunger
National Renewable Energy Laboratory, Golden, Colorado 80401
(Received 24 January 1994)

Quantum mechanical pseudopotential calculations of the absorption spectra and static dielectric constant ϵ_s of Si quantum dots with ~100–1300 atoms are presented. The predicted ϵ_s is found to be significantly reduced relative to the bulk value, but is considerably larger than the value deduced from currently available model calculations. A convenient parametrization of ϵ_s vs size R is provided. We find that for quantum dots with $R < 20$ Å the electron-hole pair is confined by the physical dimension of the dot, not by the Coulomb attraction.

PACS numbers: 77.22.Ej, 73.20.Dx, 78.66.Fd

The static dielectric constant ϵ_s,

$$\epsilon_s = 1 + \frac{2}{\pi}\int_0^\infty \epsilon_2(E)/E\,dE, \tag{1}$$

is given by the integral of the absorption spectra $\epsilon_2(E)$,

$$\epsilon_2(E) = \frac{A}{\Omega}\sum_{fi}\frac{1}{E_{fi}^2}M_{fi}^2(E)\delta(E - E_{fi}), \tag{2}$$

where $A = 8\pi^2e^2\hbar^2/3m^2$, E_{fi} is the transition energy, and $M_{fi}^2 = |\langle f|\hat{\mathbf{p}}|i\rangle|^2$ is the dipole transition matrix element between final state $|f\rangle$ and initial state $|i\rangle$, $\hat{\mathbf{p}}$ is the momentum operator, and Ω is the volume. While calculated static dielectric constants of *bulk* semiconductors [1–3] are generally in good agreement with experiment, little is known experimentally [4] or theoretically [5–8] on $\epsilon_s(R)$ for *quantum structures* whose radius R is of the order of a few lattice constants. Previous works [4–5] indicate that ϵ_s is reduced as the size R diminishes. This could have profound effects on (a) electron-hole (exciton) pairs and on (b) hydrogenic impurities: Regarding excitonic effects (a), recall that in the bulk, the free exciton radius a_{eh} scales as $a_{eh} \propto \epsilon_s$. So a strong reduction of ϵ_s from the bulk value can change the ratio $a_{eh}/2R$ from > 1 ("strong confinement" [7]) to < 1 ("weak confinement" [7]). This weak confinement behavior was recently predicted from a generalization [6] of Penn's model [9] to an isotropic, spherical semiconductor of radius R, giving

$$\epsilon_s(R) = 1 + \frac{\epsilon_b - 1}{1 + (\alpha/R)^l}, \tag{3}$$

where $l = 2$, $\alpha = 10.93$ Å in Si, and $\epsilon_b = 11.4$ is the bulk dielectric constant. This generalized Penn model (GPM) predicts (Fig. 1) that $a_{eh}/2R$ is very close to unity for all $R < 20$ Å ("weak confinement"). Regarding hydrogenic impurities (b), as ϵ_s is reduced with the particle's size we expect an enhancement in the binding energy $E_B \propto -1/\epsilon_s^2$. This could lead to an exponential reduction in free carrier density $N \sim e^{-E_B/kT}$ ("freeze-out") at temperatures T where the bulk is still conductive [6,10].

Since simple models such as Eq. (3) are of questionable validity, we provide here a *microscopic* calculation of ϵ_s vs size for nanometer silicon quantum spheres directly from Eqs. (1) and (2). The spectra $\epsilon_2(E)$ of quantum dots containing up to ~1300 Si atoms are calculated fully quantum mechanically using an empirical pseudopotential plane wave representation and a novel moments method [11]. In contrast to the GPM results [6], this atomistic calculation predicts *strong confinement* rather than *weak confinement* for $R < 20$ Å. We further provide convenient parametrization of ϵ_s vs R in the form of Eq. (3), finding, however, a considerably smaller exponent $l \approx 1.2$–1.4 than assumed earlier.

We first test our empirical pseudopotential approach for the *bulk*, calculating the absorption spectrum $\epsilon_2(E)$, the static dielectric constant ϵ_s, and the density of states. For later applications to finite clusters, a *continuous*, momentum space Si pseudopotential $v_{\mathrm{Si}}(q)$ is needed. We obtain it by fitting the bulk band structure and the surface work function [12]. The bulk absorption spectrum $\epsilon_2(E)$ was

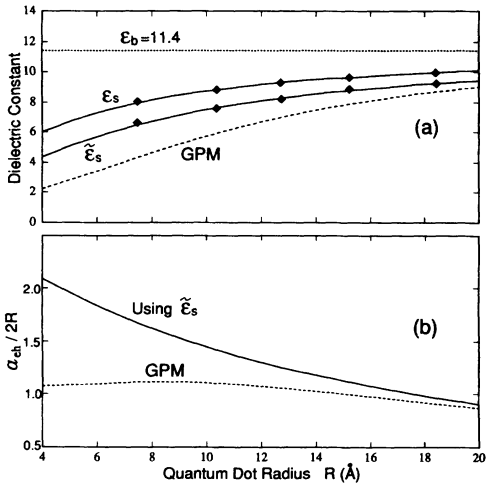

FIG. 1. Dielectric constants (a) and the ratio between the free hydrogenic exciton radius and the quantum dot diameter (b) as a function of quantum dot radius R. Here, ϵ_s is for total polarization and $\tilde{\epsilon}_s$ is for exciton screening. The diamond symbols in (a) denote the calculated results while the solid lines are the fitted curves. The dashed curve corresponds to the generalized Penn model (GPM) of Eq. (3).

0031-9007/94/73(7)/1039(4)$06.00

calculated using conventional $k \cdot p$ extrapolation methods [13] and a plane wave basis with an energy cutoff of 4.5 Ry. The results are shown in Fig. 2(a) where they are also compared with experiment [14]. While our result compares well with similar previous calculations [15], they all lack the lower energy excitonic peak apparent in the experimental spectrum. This excitonic peak cannot be described by our single particle theory. The "f-sum rule" [16] $(m\Omega/2\pi^2e^2)\int_0^\infty E\epsilon_2(E)\,dE = N$, where N is the total number of electrons inside volume Ω, is satisfied to within 0.1%. From Eq. (1) we find $\epsilon_b = 10.38$ for the bulk. This can be compared with the experimental result [17] of 11.4, the local density approximation result [2] 12.7, and the early value of Walter and Cohen [1] of 11.3. Our 10% underestimation of the experimental value probably stems from the neglect of exciton effects as well as from possible imperfections in the pseudopotential. In what follows [Fig. 1(a)], we will thus scale our calculated $(\epsilon_s - 1)$ using a factor of $(11.4 - 1)/(10.38 - 1) = 1.109$. The calculated total density of states (DOS) of the bulk Si is shown in Fig. 3(a) along with the experimental x-ray photoemission spectrum (XPS) [18]. The overall agreement is good. We conclude that we have a reasonable pseudopotential as far as the quantities of interest here $[\epsilon_2(E), \epsilon_s, \mathrm{DOS}]$ are concerned.

We next consider spherical Si quantum structures. We use interatomic distances taken from bulk since experimental Si-Si interatomic distances in quantum dots are within 0.25% of the bulk value [19]. All surface dangling bonds are saturated in our calculation by hydrogen atoms. The surface Si-Si bond relaxations and H atom positions are

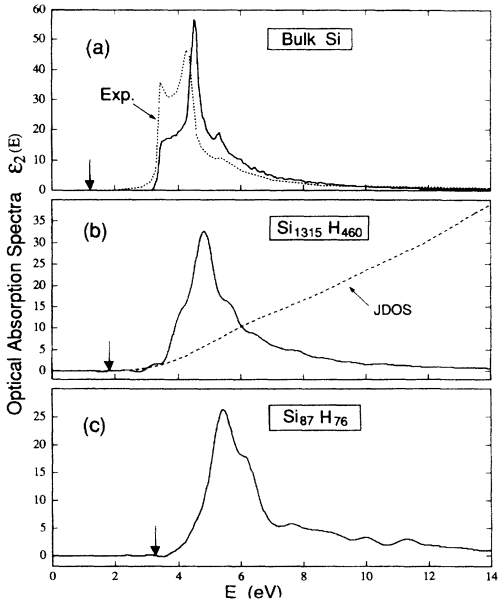

FIG. 2. Calculated optical absorption spectra $\epsilon_2(E)$ of Si systems with different sizes. The experimental data in (a) are from Ref. [14]. The joint density of states (JDOS) in (b) is given in arbitrary units. The vertical arrows denote band gap values (see Ref. [12]).

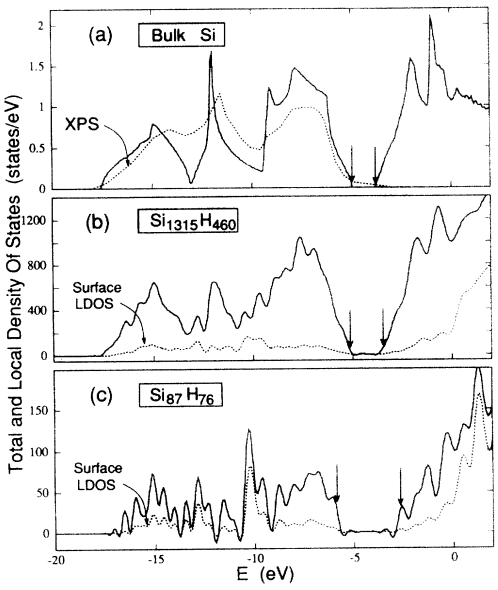

FIG. 3. Total and surface local density of states of Si systems with different sizes. The XPS data in (a) is from Ref. [18]. The vertical arrows denote band edge positions (see Ref. [12]). The zero of energy is the vacuum potential level.

modeled after experimental data and *ab initio* calculations of H-covered (100), (110), and (111) Si surfaces [12]. We believe that the error on the dielectric constant due to a possible difference between the current surface model and the real quantum dot should be small unless there are massive atomic reconstructions on the surface, about which there is currently no experimental information. The total potential $V(\mathbf{r}) = \sum_{\mathrm{atom}} v_{atom}(|\mathbf{r} - \mathbf{R}_{\mathrm{atom}}|)$ is given by a superposition of local atomic pseudopotentials of Si and H. The hydrogen pseudopotential $v_{\mathrm{H}}(r)$ is fitted [12] to the measured spectra of the above mentioned three H-covered Si surfaces. In the calculation, the quantum dots are placed in periodic unit cells with the closest distance between two neighboring quantum dots as 9 Å. The plane wave basis set energy cutoff is 4.5 Ry, corresponding to 10^5 basis functions for the largest system considered here. Such huge basis sets cannot be handled by conventional electronic structure methods that seek all eigenstates. We use instead a newly developed generalized moments method, which is summarized in the following.

The calculation of the optical spectrum

$$\epsilon_2(E) = \frac{A}{\Omega E^2}\int_{-\infty}^{E_f} dE_2 \int_{E_f}^{\infty} dE_1 \tau(E_1, E_2) \times \delta[E - (E_2 - E_1)] \qquad (4)$$

[where constant A is defined as in Eq. (2), $\Omega = N_{\mathrm{Si}}a^3/8$ is the volume, N_{Si} is the number of Si atoms, and a is the bulk Si lattice constant] requires the two-dimensional spectral function

$$\tau(E_1, E_2) = \sum_{f,i} |\langle f|\hat{\mathbf{p}}|i\rangle|^2 \delta(E_1 - E_i)\delta(E_2 - E_f). \qquad (5)$$

This is obtained here by first calculating a series of *moments* of $\tau(E_1, E_2)$ and then linearly transforming them to energy space. The moments are conveniently expressed in a basis of orthogonal Chebychev polynomials T_n. To obtain them we use randomly generated wave function $|\psi_0\rangle$, calculating

$$\Gamma_{n,m} = \langle\psi_0|\hat{\mathbf{p}}T_n(\hat{H}) \cdot \hat{\mathbf{p}}T_m(\hat{H})|\psi_0\rangle, \quad (6)$$

where $\hat{H}$ is the system's Hamiltonian with its energy scaled so that all its eigenvalues fall inside domain $[-1:1]$. Taking an ensemble average over $\Gamma_{n,m}$ using different, randomly generated $|\psi_0\rangle$'s gives the required moments of $\tau(E_1, E_2)$:

$$\langle\Gamma_{n,m}\rangle = \int_{-1}^{1} dE_1 \int_{-1}^{1} dE_2 T_n(E_1)\, T_m(E_2)\, \tau(E_1, E_2). \quad (7)$$

The function $\tau(E_1, E_2)$ can then be reconstructed as

$$\tau(E_1, E_2) = \left(\frac{2}{\pi}\right)^2 (1 - E_1^2)^{-1/2} (1 - E_2^2)^{-1/2} \times \sum_{n,m} T_n(E_1)\, T_m(E_2) \langle\Gamma_{n,m}\rangle \times (1 + \delta_{n0})^{-1} (1 + \delta_{m0})^{-1}, \quad (8)$$

using the orthogonality of T_n. We use in the present calculations 500×500 Chebychev moments $\Gamma_{n,m}$ and 5–60 randomly selected wave functions $|\psi_0\rangle$. The total and local density of states can be calculated analogously. Numerical details of this method are given elsewhere [11].

We consider five spherical quantum dots: $Si_{87}H_{76}$, $Si_{235}H_{140}$, $Si_{429}H_{228}$, $Si_{741}H_{300}$, and $Si_{1315}H_{460}$. The calculated spectra $\epsilon_2(E)$ of the smallest and the largest quantum dots are given in Figs. 2(b) and 2(c), while the total and local density of states are shown in Figs. 3(b) and 3(c).

The results exhibit the following features: (i) The band gaps (marked in Fig. 2 by vertical arrows) and peaks of $\epsilon_2(E)$ shift to higher energies with decreasing size, as expected from quantum confinement. The size scaling of the band gap change is, however, $\Delta E_g(R) \sim R^{-n}$ with $n = 1.4$, not the $n = 2$ exponent expected from simplistic particle-in-a-box effective mass models. (ii) $\epsilon_2(E)$ and the DOS of the largest quantum dot studied here already resemble their bulk counterparts, while the smaller particles have fundamentally different characteristics. (iii) As seen in Figs. 3(b) and 3(c), chemisorption effects are noticeable for the smaller cluster: Surface Si-H bonding produces a peak in DOS at about 5 eV *below* the valence band maximum. The band gap region, however, has no surface state. (iv) Comparing [Fig. 2(b)] ϵ_2 with the joint density of state (JDOS) shows that the dipole matrix element M_{fi}/E_{fi} controls the shape of the absorption spectra. A constant matrix element approximation (i.e., equating ϵ_2 with the JDOS) is obviously useless here.

Integrating $\epsilon_2(E)$ of Fig. 2 according to Eq. (1) gives the *total polarization dielectric constant* $\epsilon_s(R)$ depicted in Fig. 1(a). This measures the total polarization $\mathbf{P}$ of a system of volume Ω, responding to a constant electric field $\mathbf{F}$, i.e., $\epsilon_s \equiv 1 + \mathbf{P}/\mathbf{F}\Omega$. This total polarization $\mathbf{P}$ consists of contributions from the interior Si atoms, as well as from the surface Si-H bonds. The magnitudes of these contributions can be estimated from Penn's model using

$$\epsilon_s - 1 \approx \frac{4\pi e^2}{m\Omega}\left[\frac{4N_{\mathrm{Si}} - N_{\mathrm{H}}}{E_{\mathrm{Si}}^2} + \frac{2N_{\mathrm{H}}}{E_{\mathrm{Si-H}}^2}\right], \quad (9)$$

where $4N_{\mathrm{Si}} - N_{\mathrm{H}}$ and $2N_{\mathrm{H}}$ are the numbers of electrons in Si-Si and Si-H bonds, respectively. Neglecting (on purpose) the size dependence (i.e., the quantum confinement effect) of $E_{\mathrm{Si}}(R)$, we find $E_{\mathrm{Si}} = 5.15$ eV [taken from bulk value, i.e., $N_{\mathrm{H}} = 0$, $\epsilon_s = \epsilon_b$ in Eq. (9)] and $E_{\mathrm{Si-H}} = E_{\mathrm{Si}}/2 + 5.6$ eV, where –5.6 eV is the Si-H peak position in LDOS of Fig. 3 measured from the center of the band gap. The dot-interior and surface contributions to $\epsilon_s - 1$ [first and second terms of Eq. (9), respectively] are then $9.5 + 0.7 (= 10.2)$, $9.3 + 0.8 (= 10.1)$, $9.0 + 1.1 (= 10.1)$, $8.8 + 1.2 (= 10.0)$, and $8.1 + 1.8 (= 9.9)$, for the quantum dots $Si_{1315}H_{460}$, $Si_{741}H_{300}$, $Si_{429}H_{228}$, $Si_{235}H_{140}$, and $Si_{87}H_{76}$, respectively. We see that (i) even though the surface-to-volume ratio increases as the dot gets smaller, most of ϵ_s comes from the dot-interior Si atoms, not the surface. (ii) The model $\epsilon_s - 1$ estimated from Eq. (9) is almost size independent, being close to the bulk value 10.4. Thus the large reduction of ϵ_s with size noted in our *direct* calculation of Fig. 1(a) cannot be explained in terms of surface effect, and must reflect quantum confinement effects.

Another interesting quantity is the *screening dielectric constant* $\tilde{\epsilon}_s(R)$ which effectively measures the reduction in the Coulomb potential of an electron or hole due to screening by the medium. Because of the wave vector (q) dependence of the bulk dielectric function $\epsilon_b(q)$ and the small dimension of the quantum dots, we expect $\tilde{\epsilon}_s(R) < \epsilon_s(R)$. There is no unique definition of $\tilde{\epsilon}_s$ since this quantity can depend on the specific potentials to be screened. Here, we define $\tilde{\epsilon}_s$ from a model exciton wave function [20], so the results are most appropriate to describe exciton screening and exciton binding energy in nanostructures [20].

For a spherical quantum dot with radius R, the charge density of an uncorrelated electron or hole is [20]

$$\rho(r) = \left[\left(\frac{\pi}{2R^3}\right)^{1/2} \frac{\sin(\frac{\pi}{R}r)}{\frac{\pi}{R}r}\right]^2 \quad \text{for } r \le R, \quad (10)$$

and zero elsewhere. This produces an unscreened external potential $v_{ext}(r)$ obtained from $\rho(r)$ by solving Poisson's equation with a boundary condition $v_{\mathrm{ext}}(R) = 0$. Then, if there exists a *"macroscopic"* screening ϵ (no q dependence or local field effect) inside the sphere, the ensuing screened potential for $r \le R$ is $v_{\mathrm{scr}}(r) = v_{\mathrm{ext}}(r)/\epsilon$. For a *microscopic* screening, $v_{\mathrm{ext}}(r)$ and $v_{\mathrm{scr}}(r)$ are not proportional. In that case, we can define $\tilde{\epsilon}_s$ as the ratio between the unscreened and screened Coulomb energies $\tilde{\epsilon}_s = \int v_{\mathrm{ext}}(r)\rho(r)\, d^3r / \int v_{\mathrm{scr}}(r)\rho(r)\, d^3r$. To simplify the calculation, we will replace the truly external potential

$v_{ext}(r)$ by $v'_{ext}(r)$, which generates (after being screened by the medium) a screened potential $v'_{src}(r) = v_{ext}(r)$. We then have

$$\tilde{\epsilon}_s = \int v'_{ext}(r)\rho(r)\,d^3r \Big/ \int v'_{src}(r)\rho(r)\,d^3r\,. \qquad (11)$$

With this definition, using perturbation theory, we find that:

$$\tilde{\epsilon}_s = 1 + \frac{2}{\pi}\int_0^\infty \frac{\tilde{\epsilon}_2(E)}{E}\,dE\,, \qquad (12)$$

and

$$\tilde{\epsilon}_2(E) = \frac{2\pi}{\beta}\sum_{f,i}|\langle f|v_{ext}(r)|i\rangle|^2\delta(E - E_{fi})\,, \qquad (13)$$

where $\beta \equiv \int v_{ext}(r)\rho(r)\,d^3r$. Thus, $\tilde{\epsilon}_2$ can be calculated in the same way as the spectrum ϵ_2, replacing, however, the momentum operator $\hat{\mathbf{p}}$ in Eqs. (5) and (6) by the external potential $v_{ext}(r)$.

The calculated screening dielectric constants $\tilde{\epsilon}_s$ for the spherical clusters are plotted in Fig. 1(a). As expected, $\tilde{\epsilon}_s(R)$ is smaller than $\epsilon_s(R)$. At the same time, it is still larger than the value predicted by the GPM. Consequently, the ratio $(a_{eh}/2R)$ between the bulklike (free) hydrogenic exciton radius and the system's size is predicted to be far larger than unity for $R < 20$ Å (strong confinement), as shown in Fig. 1(b).

It is useful to have a simple analytical form for the dielectric constant vs size. Fitting our results to the analytic form of Eq. (3) gives the solid lines shown in Fig. 1(a). We find $\alpha = 4.25$ Å, $l = 1.25$ Å for the *total polarization dielectric constant* ϵ_s, and $\alpha = 6.9$ Å, $l = 1.37$ Å for the *screening dielectric constant* $\tilde{\epsilon}_s$. The GPM gives $\alpha = 10.93$ and $l = 2$. The fact that our $l < 2$ is reminiscent of the fact that we also find a band gap scaling $\sim 1/R^n$ with a softer exponent $n \sim 1.4$ than the effective mass $n = 2$ value.

A sensitive test of the size dependence of $\tilde{\epsilon}_s(R)$ is to compare with experiment the calculated ratio between the conduction band edge shift $[\Delta E_c(R) \equiv E_c(R) - E_c(\infty)]$ and the valence band edge shift $[\Delta E_v(R) \equiv E_v(\infty) - E_v(R)]$. Because this type of experiment [21] does not require measurement of the size of the quantum dots, it avoids the large uncertainty encountered in conventional experiments which measure $\Delta E_{gap}(R)$ as a function of R. The measured conduction band energy contains an exciton Coulomb energy term. This Coulomb energy can be calculated [20] by a simple formula $-1.786/\epsilon R$. As shown in Fig. 4, using the present $\tilde{\epsilon}_s(R)$ rather than the bulk value ϵ_b for ϵ brings the calculated ΔE_c vs ΔE_v results much closer to the experimental data. Interestingly, using the GPM values of $\epsilon(R)$ gives results which are at the other side of the experimental data range.

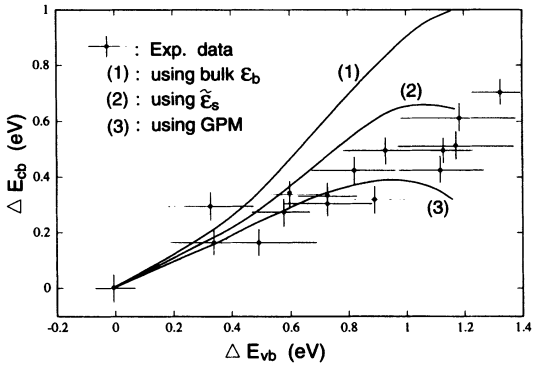

FIG. 4. Conduction band edge shifts versus valence band edge shifts. The experimental data are from Ref. [21].

This work was supported by the office of Energy Research, Materials Science Division, U.S. Department of Energy, under Grant No. DE-AC02-83CH10093.

[1] J.P. Walter and M.L. Cohen, Phys. Rev. B **2**, 1821 (1970).
[2] S. Baroni and R. Resta, Phys. Rev. B **33**, 7017 (1986).
[3] M.S. Hybertsen and S.G. Louie, Comments Condens. Matter. Phys. **13**, 273 (1987), and references herein.
[4] J.F. Harvey, H. Shen, R.A. Lux, M. Dutta, J. Pamulapati, and R. Tsu, Mater. Res. Soc. Symp. Proc. **256**, 175 (1992).
[5] K.B. Kahen, J.P. Leburton, and K. Hess, Superlattices Microstruct. **1**, 289 (1985); R. Tsu and L. Ioriatti, *ibid.* **4**, 295 (1985).
[6] R. Tsu, L. Ioriatti, J.F. Harvey, H. Shen, and R.A. Lux, Mater. Res. Soc. Symp. Proc. **283**, 437 (1993).
[7] A.D. Yoffe, Adv. Phys. **42**, 173 (1993).
[8] G. Mie, Ann. Phys. (Leipzig) **25**, 377 (1908); P. Debye, *ibid.* **30**, 57 (1909).
[9] D.R. Penn, Phys. Rev. **128**, 2093 (1962).
[10] J.F. Harvey, R.A. Lux, D.C. Morton, G.F. Mclane, and R. Tsu, Mater. Res. Soc. Symp. Proc. **283**, 395 (1993).
[11] L.W. Wang, Phys. Rev. B **49**, 10154 (1994).
[12] For detail pseudopotential fitting and quantum dot atomic structures, see L.W. Wang and A. Zunger, J. Phys. Chem. **98**, 2158 (1994).
[13] D. Buss and N.J. Parada, Phys. Rev. B **1**, 2692 (1970).
[14] D.E. Aspnes and A.A. Studna, Phys. Rev. B **27**, 985 (1983); G.E. Jellison, Jr. and F.A. Modine, *ibid.* **27**, 7466 (1983).
[15] M.L. Cohen and J.R. Chelikowsky, *Electronic Structure and Optical Properties of Semiconductors* (Springer-Verlag, Berlin, 1988).
[16] M. Altarelli, D.L. Dexter, and H.M. Nussenzveig, Phys. Rev. B **6**, 4502 (1972).
[17] R.A. Faulkner, Phys. Rev. **184**, 713 (1969); H.W. Icenogle, B.C. Platt, and W.L. Wolfe, Appl. Opt. **15**, 2348 (1976).
[18] L. Ley, S.P. Kowalczyk, R.A. Pollak, and D.A. Shirley, Phys. Rev. Lett. **29**, 1088 (1972).
[19] K.A. Littau, P.J. Szajowski, A.J. Muller, A.R. Kortan, and L.E. Brus, J. Phys. Chem. **97**, 1224 (1993).
[20] L.E. Brus, J. Phys. Chem. **90**, 2555 (1986).
[21] T. van Buuren, T. Tiedje, J.R. Dahn, and B.M. Way, Appl. Phys. Lett. **63**, 2911 (1993).